Microvascular Photodynamic Effects Determined *In Vivo* Using Optical Doppler Tomography

Attila Major, S. Kimel, Steven Mee, Thomas E. Milner, Derek J. Smithies, Shyam M. Srinivas, Zhongping Chen, and J. Stuart Nelson

***Abstract*— Vascular responses were monitored to understand the role of the microvasculature in tumor destruction as a result of photodynamic therapy (PDT). Rats received an intravenous dose of 2 mg/kg Benzoporphyrin Derivative (BPD), at 20 min, 4 h, or 7 h before laser irradiation. With Photofrin (10 mg/kg), drug-light intervals were 20 min or 8 h. Jejunal blood vessels were exposed to 12 J/cm^2 at 690 nm (with BPD) or at 630 nm (with Photofrin). Optical Doppler tomography (ODT) was used to evaluate PDT-induced changes in vessel diameter and blood flow. At the shortest drug-light time interval (20 min), BPD-mediated PDT caused transient constriction of arteries, accompanied by decreased blood flow, followed by vasodilation until baseline was reached or overshoot occurred. Veins became occluded with no restoration of the vessel lumen. At longer drug-light intervals, vasoconstriction diminished and venodilation was observed. With Photofrin, vasoconstriction and venodilation increased with the drug-light interval. Application of a higher light dose (48 J/cm^2) resulted in irreversible hemostasis. ODT can be used to study changes in lumen diameter and blood flow, which are important diagnostic parameters of PDT.**

***Index Terms*— Blood flow imaging, mechanistic photochemotherapy, optical coherence tomography, rat jejunal mesentery, transient vascular effects, vasoconstriction, venodilation.**

I. Introduction

PHOTODYNAMIC therapy (PDT) is an experimental modality for treatment of cancer [1], [2] and diseases related to vascular integrity [3]–[10]. In PDT, a photosensitizing drug is usually administered systemically, and over time becomes preferentially retained in tumor tissue. When the ratio of photosensitizer accumulation in cancerous versus surrounding-host-tissue is optimal, the tumor area is exposed to an appropriate light dose, in the therapeutic spectral window between 630–800 nm, at a selected wavelength coinciding with an absorption peak of the photosensitizer. Photoexcitation of sensitizer molecules, followed by energy transfer to tissue oxygen, leads to generation of short-lived, reactive oxygen species (ROS) that cause oxidative damage to intracellular target molecules. Depending on the photosensitizer and the relevant drug-light time interval, the ensuing cytotoxicity elicits tumor regression, either directly by tumor cell inactivation [11], [12] and/or indirectly by damaging endothelial cells, leading to destruction of the microvasculature nourishing the tumor [13]. In particular, if the targeted area is exposed to light shortly after drug administration, when drug concentration in blood is high, a strong vascular response is expected.

In systemic PDT, the vascular pathway is widely considered to be the prominent mechanism for tumor destruction, as shown by histology [14], blood flow measurement [15]–[19], sandwich observation chambers [13] and fluorescence kinetics [20]. Stasis of tumor blood flow shortly after initiation of PDT has been inferred from measuring tissue oxygen depletion during laser irradiation [21]. Histopathological studies show that thrombus formation and hemostasis are common occurrences following PDT in experimental animals and humans [14]. These observations suggest that tumor necrosis results primarily from destruction of the microvasculature nourishing the tumor tissue. Thus, the endothelium/vasculature represents an important target, and monitoring intratumoral blood flow can assess progress of PDT.

The dependence of vascular effects on drug, light, and drug-light time interval (Δt) has been studied intensively [1], [2], [17], [22] in an attempt to better understand tumor destruction and curative effects, so far with limited success. An important factor that has hindered progress is the absence of a quantitative tomographic imaging modality that may be used to assess vascular anatomical changes in real time in response to PDT.

In rat jejunal mesentery, a decrease of blood flow was reported following hematoporphyrin derivative mediated PDT [23], [24]. Histologic [14] and microscopic observations [14] in various animal models have shown that PDT leads to destructive vascular effects such as thrombosis, thromboxane release by activated platelets [16], endothelial cell membrane damage [25], or vascular leakage and constriction [16]–[18]. Loss of vessel wall integrity usually follows, producing tissue ischemia and subsequent necrosis [13].

Manuscript received February 4, 1999; revised July 2, 1999. This work was supported by awards from the Whitaker Foundation under Research Grant 21025 and Research Grant 23281, and by the Institute of Arthritis and Musculoskeletal and Skin Diseases at the National Institutes of Health under Grant 1RO1 AR43419-01A and by the Institute of Heart, Lung, and Blood at the National Institutes of Health under Grant 1R01HL/GM59472-05. This work was supported by the Office of Naval Research under Contract N00014-94-1-0874, by the Department of Energy under Contract DE-FG03-91ER61227, by the National Institutes of Health under Grant RR-01192, and by an Endowment from the Beckman Laser Institute and Medical Clinic. The work of A. Major was supported by the Hermann Klaus Foundation, Zürich, Switzerland. The work of S. Kimel was supported by the U.S.–Israel Binational Science Foundation under Grant 93-00154, Jerusalem, Israel.

A. Major is with the Department of Obstetrics and Gynecology, University Hospital, Zürich, Switzerland.

S. Kimel is with the Beckman Laser Institute and Medical Clinic, University of California, Irvine, CA 92612 USA. He is also with the Department of Chemistry, Technion-Israel Institute of Technology, Haifa 32000, Israel.

S. Mee, D. J. Smithies, S. M. Srinivas, Z. Chen, and J. S. Nelson are with the Beckman Laser Institute and Medical Clinic, University of California, Irvine, CA 92612 USA.

T. E. Milner is with the Biomedical Engineering Program, The University of Texas at Austin, Austin, TX 78712 USA.

Publisher Item Identifier S 1077-260X(99)07542-5.

Due to past technical limitations, transient changes *in vivo* were difficult to observe so that the mechanism(s) underlying vascular effects have remained incompletely understood [26]. Vascular events in PDT occur on a time scale of minutes and biophysical events that trigger early changes cannot be identified by histologic observations after the fixation processes. These events involve PDT-mediated perturbations of both endothelial and hematological factor release cascades. *In vivo* quantitative observation of both vessel size and intraluminal blood flow may lead to new insights into the cause of vascular damage by PDT [15]–[19]. Presently, optical Doppler tomography (ODT) is not able to reveal directly functional information regarding the cellular and biochemical changes that occur during PDT.

We have used ODT for simultaneous determination of vessel diameters, with micrometer scale resolution, and blood flow velocity profiles, on the order of 100 μm/s, observed acutely during a 1-h observation period following laser irradiation in PDT.

II. Materials and Methods

Benzoporphyrin derivative monoacid ring A (BPD) was obtained from QLT (Vancouver, Canada). The liposomal powder was reconstituted with sterile water to a concentration of 2 mg/ml. Photofrin® in the form of porfimer sodium powder, also obtained from QLT, was dissolved in 5% dextrose to a concentration of 2.5 mg/ml.

The rodent jejunal mesentery was selected for study of PDT-induced vascular effects. This animal model enables investigation of an adjacent artery and vein pair, having diameters in the range of 100–300 μm, with opposing blood flow directions. The model provides information on anatomical features and blood flow velocities to an accuracy that can only be measured with ODT.

A total of 17 mature Sprague-Dawley female rats (250–350 g) were housed in a pathogen free animal facility and given a commercial base diet and water ad libitum. The experimental protocol was approved by the Institutional Animal Care and Use Committee at the University of California, Irvine. Animals were anesthetized with an intramuscular injection of ketamine (87 mg/kg) and xylazine (13 mg/kg). The animal was placed in the supine position on a temperature-controlled heating pad and a midline laparotomy incision of 2 cm (xyphoid to pubic symphysis) was made. A segment of jejunum was mobilized outside the abdomen to expose the mesenteric blood vessels and minimize effect of respiratory movement on recorded data. First, exploratory ODT scans were performed to identify a suitable vessel pair, which was marked by dissecting away mesenteric fat on either side of the vessels. The exposed tissue was periodically irrigated with isotonic saline to prevent desiccation. When laser irradiation was performed after longer time intervals ($\Delta t = 4, 7, 8$ h) the abdominal walls were sutured and later reopened for PDT and subsequent ODT measurements. Also, at the longer intervals, physiological saline (10 ml) was injected subcutaneously in order to compensate for fluid loss. After the last ODT measurement, animals were given intracardiac injections of Euthanasia-6 (Western Medical Supply, Arcadia, CA).

After preselected time intervals (Δt) PDT was performed on the exposed mesentery. With BPD, radiation at 690 nm was provided by a diode laser (Lawrence Livermore Laboratories, Livermore, CA), equipped with a microlens-terminated multimode optical fiber, at a uniform power density of 100 mW/cm^2, 2 cm diameter spot, 120 s treatment duration, giving a light dose $D = 12$ J/cm^2. With Photofrin, radiation at 630 nm from an Innova model 90 argon–ion and a model 599 dye laser system (Coherent, Palo Alto, CA) was delivered at a uniform power density of 100 mW/cm^2, 2 cm diameter spot, 120 or 480 s treatment duration, corresponding to a light dose $D = 12$ J/cm^2 or $D = 48$ J/cm^2.

The first group of animals received BPD (2 mg/kg body weight) by tail vein injection, at specified time intervals ($\Delta t = 20$ min $(n = 3)$, 4 h $(n = 3)$ or 7 h $(n = 3)$) prior to laser irradiation ($D = 12$ J/cm^2). The second group received i.v. doses of Photofrin (10 mg/kg body weight), at $\Delta t = 20$ min $(n = 2)$ or $\Delta t = 8$ h $(n = 2)$ prior to laser irradiation ($D = 12$ J/cm^2); in addition, one animal received a higher light dose ($D = 48$ J/cm^2) at $\Delta t = 20$ min $(n = 1)$. Animals in the control group $(n = 3)$ received an i.v. bolus of 1 ml physiological saline and, at $\Delta t = 20$ min, were irradiated with 690 nm radiation ($D = 12$ J/cm^2).

ODT is a recently developed technique that combines optical low coherence tomography with Doppler velocimetry for the purpose of real-time imaging, with high spatial resolution, of structure as well as flow velocity in biological specimens. ODT instrumentation has been described in detail previously [27]–[30]. Briefly, a He–Ne aiming laser ($\lambda = 632.8$ nm, 1 μW, spot-size 100 μm^2) and a broad-band superluminescent diode (SLD) source ($\lambda_0 = 850$ nm, bandwidth $\Delta\lambda = 25$ nm, 1 mW) were coupled into a fiber-optic Michelson interferometer and split by a $2x \times 2$ fiber coupler into reference and sample beams (Fig. 1). The optical path lengths of light in the reference and sample beams were modulated (at a frequency $f = 1.6$ kHz) with two piezoelectric cylinders around which the optical fibers were wrapped. To provide a velocity component of blood constituents along the incident light propagation direction, the sample beam was incident on the mesentery at about 15° from the tissue-surface normal. Light backscattered from the mesentery and collected by the sample fiber was recombined and mixed with the retroreflected reference beam in the 2×2 coupler. Interference fringes were observed only when the path length difference between the sample and reference beams was within the source coherence length. The sample beam was positioned outside the artery–vein pair, and prior to scanning the He–Ne laser was blocked. The optical energy delivered to the sample by the He–Ne aiming beam (<1 J/cm^2) was thus maintained below threshold to prevent induction of any PDT-mediated artifacts that might occur, specifically when using Photofrin. Because the optical dose due to the He–Ne laser was below threshold, no control group of animals was studied to investigate vascular effects resulting from exposure to the aiming beam alone. The sample beam was translated laterally, parallel to the tissue surface (at a speed of ~700 μm/s) within the x, z plane over a distance of 1200–1500 μm, and displaced at incremental depths z (~10 μm), to form a raster scan covering about 100

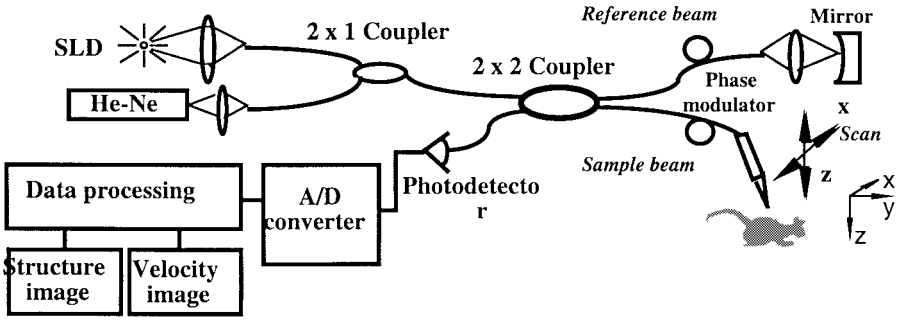

Fig. 1. Schematic of ODT instrumentation.

increments. The longitudinal spatial resolution (perpendicular to the tissue surface) of ODT is determined by the coherence length (l_c) of the source

$$l_c = \frac{4\ \ln\ 2}{n\pi}\ \frac{\lambda^2}{\Delta\lambda} \tag{1}$$

where n is the refractive index of the tissue (taken to be $n = 1.4$), so that (for $\lambda = 0.85\ \mu$m and $\Delta\lambda = 0.025\ \mu$m) $l_c = 18\ \mu$m. Lateral spatial resolution of ODT instrumentation was limited by the numerical aperture (0.20) of the focussing lens in the sample arm and was approximately 5 μm. The longitudinal and lateral spatial resolution of the ODT system is thought to be independent of image depth and lateral scanning speed.

The time required to record a single pixel in structural and Doppler velocity images was $\tau = 12.5$ ms, which determined the minimal relative velocity resolution (ΔV) as given by

$$\Delta f = \frac{2\cos\theta}{\lambda}\Delta V \tag{2}$$

Here Δf denotes the resolvable Doppler shift (Hz) which is inversely proportional to the pixel acquisition time τ, and θ is the angle between the red blood cell (RBC) flow velocity and the incident beam. For $\Delta f = 80$ Hz and $\theta = 75°$, we obtain $\Delta V = 130\ \mu$m/s.

The instrument employed in this study limited the data collection for a complete scan to about once every 5 min. Interference fringe intensity was measured with a silicon photodiode and digitized with a 16-bit A/D converter. The acquired data were transferred to a computer work station for further processing. The interference fringes at each pixel were transformed using a short-time fast Fourier transform spectrogram. Unshifted interference fringe intensity (i.e., at $f = 1.6$ kHz) of backscattered light from static structures was used to form a structural image. Because of RBC's moving parallel to the tissue surface in a direction having a component along the incident sample beam, in the structural image of a vessel, light backscattered from flowing blood was Doppler-shifted out of the detection window and appeared dark. The flow image was obtained from light backscattered from moving constituents (e.g., RBC's). The Doppler shift of that light was determined by computing the deviation of the first moment of the interference fringe intensity frequency spectrum from the phase modulation frequency (1.6 kHz) established by the piezoelectric modulators. Gray-scale values were assigned to each pixel in the blood flow velocity images according to magnitude of the computed Doppler shift. Lighter shades in the blood flow velocity image correspond to RBC's having higher velocities. Simultaneous measurements of interference fringe intensity and Doppler frequency shift allowed construction of cross-sectional structural and blood flow velocity images, respectively.

The spatial resolution of ODT [18 μm, see (1)] is an order of magnitude better than what can be achieved with ultrasound tomography [31]. Vessels positioned within hundreds of micrometers beneath the tissue surface with diameters as small as 10 μm can be imaged with ODT. Similarly, the relative velocity resolution in ODT [130 μm/s, see (2)] is better than in ultrasound because of the difference in the respective wavelengths. A detailed investigation of ODT velocity resolution limitations has been conducted using Monte Carlo simulations of light propagation in tissue [32]. For ultrasound, $\lambda_{\text{acoustic}}$ depends on the wave frequency and mean velocity of sound through soft tissue (taken to be 1540 m/s). For 10-MHz ultrasound, $\lambda_{\text{acoustic}} = [1540\ \text{(m/s)}/10^7\ \text{Hz}] = 154\ \mu$m compared to $\lambda_{\text{optic}} = 0.85\ \mu$m. Assuming equal measurement time (τ) to record a single pixel in acoustic and optical Doppler imaging systems, the ratio of velocity resolutions is given by [see (2), which is valid for both ODT and ultrasound]

$$\Delta V_{\text{acoustic}}/\Delta V_{\text{optic}} = \lambda_{\text{acoustic}}/\lambda_{\text{optic}} = [154/0.85] = 180$$

This two-order of magnitude improvement in ΔV, together with the tenfold improvement in ODT spatial resolution, allow measurement of volumetric blood flow rates on the order of 10–100 pl/s.

A custom software utility was written and incorporated into the commercial computer software package AVS (Application Visualization System, Waltham MA) [33] to analyze and display recorded data. This software enabled us to compute the area of the lumen in either structural or Doppler images and to determine the mean flow velocity (average over each pixel element within the lumen).

The light-exposed segments of the mesenteric vessels were imaged and blood flow measured immediately post-irradiation $(t = 0)$ and at 6 or 7 time points, t, later. Technical limitations in data acquisition prevented image formation at the identical time points t for each animal.

III. Results

Figs. 2 and 3 present typical structural tomographic images of a vessel pair in the rat jejunal mesentery, at three selected post-irradiation time points following BPD-mediated PDT

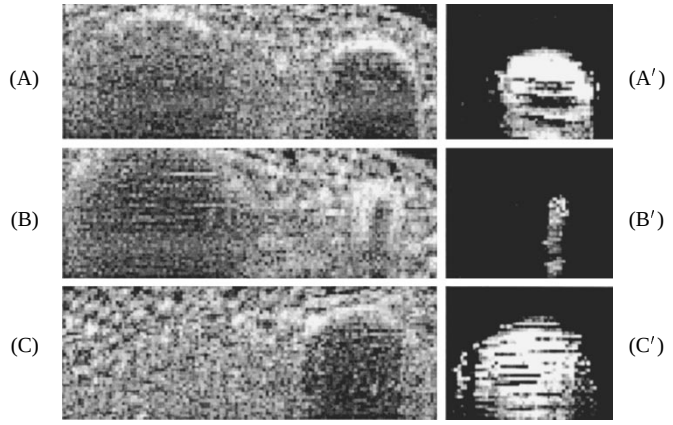

Fig. 2. Structural images of rodent mesentery artery (right) and vein (left) following BPD-mediated PDT ($\Delta t = 20$ min), at three time points post-irradiation. (A) ($t = 0$ min), (B) ($t = 16$ min), and (C) ($t = 61$ min). Note complete occlusion of vein in C. Corresponding blood velocity images of arterial blood flow are designated (A′), (B′), and (C′). In ODT, venous blood flow is poorly defined and not shown here. (1 mm = 20 μm.)

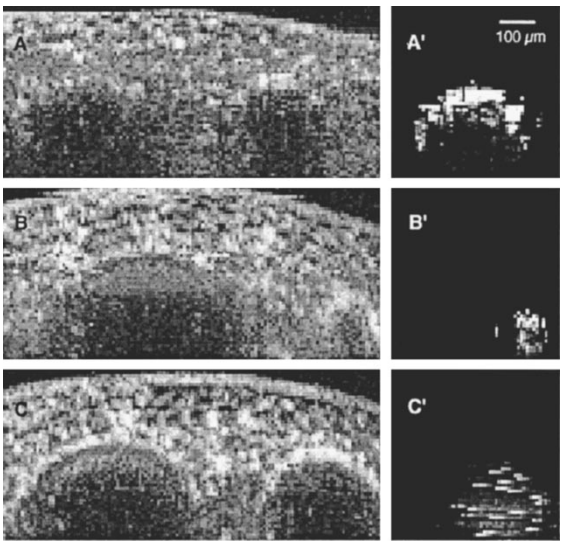

Fig. 3. Structural images of rodent mesentery artery (right) and vein (left) following Photofrin-mediated PDT ($\Delta t = 8$ h), at three time points post-irradiation. (A) ($t = 0$ min), (B) ($t = 11$ min), and (C) ($t = 51$ min). Corresponding blood velocity images of arterial blood flow are designated (A′), (B′), and (C′). In ODT, venous blood flow is poorly defined and not shown here. (1 mm = 20 μm.)

and Photofrin-mediated PDT, respectively. Arterial (d_a) and venous lumen diameters (d_v) range from 100–300 μm. ODT structural and blood flow velocity images of arterioles in the scanned x, z cross-sectional plane are also shown in Figs. 2 and 3. At the artery center, a lighter shade indicates maximal flow velocity, which decreases radially toward the vessel wall. Dark regions near the vessel center are due to blood pulsation. Given the constraints of the phase modulation scheme in the ODT instrumentation, measurements of low venous blood flow velocities were unreliable. The complete data, generated from custom AVS software utilities, are presented in Figs. 4–6.

Fig. 4 summarizes results obtained with BPD. Fig. 4(a) depicts percent changes of $d_a(t)$, relative to the value $d_a(0)$, at six post-irradiation time points, for short ($\Delta t = 20$ min), intermediate ($\Delta t = 4$ h), and long ($\Delta t = 7$ h) drug-light time intervals. Similarly, Fig. 4(b) indicates percent changes in the

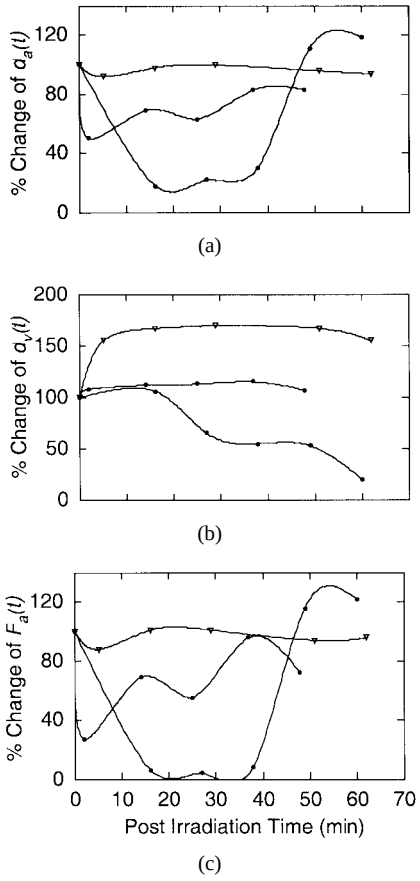

Fig. 4. BPD-mediated vascular changes due to PDT performed after three drug-light time intervals Δt as a function of post-irradiation time t. (a) Relative artery lumen diameters. (b) Relative vein lumen diameters. (c) Relative mean arterial flow. ○: $\Delta t = 20$ min. □: $\Delta t = 4$ h. ◇: $\Delta t = 7$ h ($D = 12$ J/cm^2).

venous lumen diameter $d_v(t)/d_v(0)$ versus observation time. Fig. 4(c) depicts the percent changes in the arterial volumetric blood flow rate, $F_a(t)/F_a(0)$, where $F_a(t)$ was derived from the product of the arterial lumen cross-sectional area and the mean arterial velocity at the specific time point t. Post-irradiation effects in the arteries depended dramatically on Δt. For $\Delta t = 20$ min, $d_a(t)$ decreased by 80% (at $t = 15$ min) followed by rebound, with vasodilative overshoot for $t > 40$ min. As for the vein, after an initial delay ($t > 12$ min) d_v decreased monotonically, resulting in complete occlusion. For $\Delta t = 4$ and 7 h, vasoconstriction progressively diminished, whereas the veins showed venodilation.

Results with Photofrin for short ($\Delta t = 20$ min) and long ($\Delta t = 8$ h) drug-light time intervals are given in Fig. 5. At $\Delta t = 8$ h, d_a decreased rapidly and to a greater degree than at $\Delta t = 20$ min, but returned to baseline at $t > 40$ min. In contrast, for $\Delta t = 20$ min $F_a(t)$ remained low. Fig. 6 compares results with Photofrin at $\Delta t = 20$ min for "low" and "high" fluence values. At $D = 48$ J/cm^2, arteries and veins collapsed irreversibly.

Curves recorded for the same Δt in Figs. 4 and 5 represent an individual test animal, as do the curves recorded for 12 and 48 J/cm^2 (Fig. 6). Measurements were repeated with several rats on different days, but the data do not warrant performing an error analysis. While we are confident of the qualitative

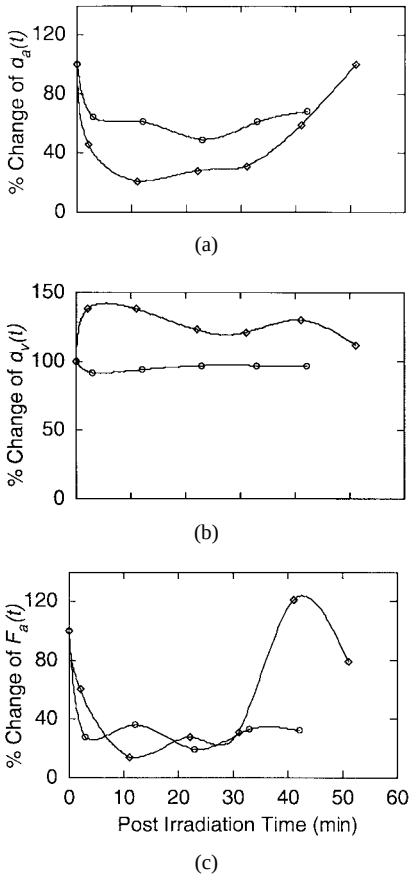

Fig. 5. Photofrin-mediated vascular changes due to PDT performed after two drug-light time intervals Δt as a function of post-irradiation time t. (a) Relative artery lumen diameters. (b) Relative vein lumen diameters. (c) Relative mean arterial flow. ○: $\Delta t = 20$ min. ◇: $\Delta t = 8$ h ($D = 12$ J/cm^2).

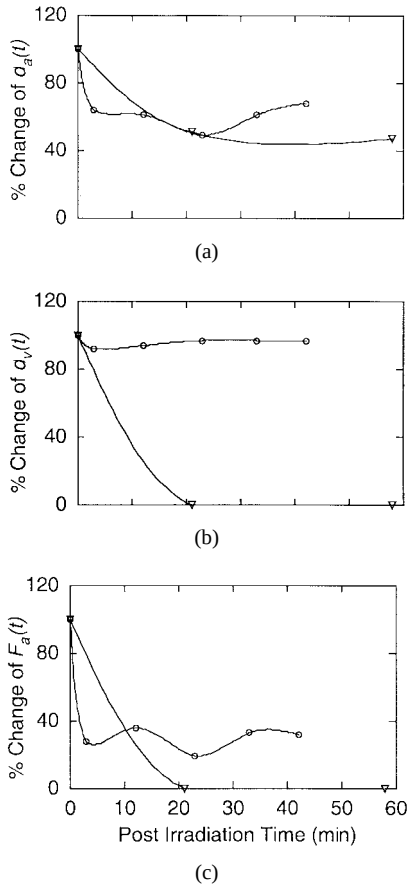

Fig. 6. Photofrin-mediated vascular changes at $\Delta t = 20$ min for two light doses. ○: $D = 12$ J/cm^2. ▽: $D = 48$ J/cm^2. (a) Relative artery lumen diameters. (b) Relative vein lumen diameters. (c) Relative mean arterial flow.

nature of the results, they are quantitatively accurate only to within ±10%. In control animals, no significant changes in $d_a(t), d_v(t)$, and $F_a(t)$ were observed (results not shown).

IV. Discussion

Using the noncontact ODT method, vessel diameter and blood flow velocity were imaged quantitatively *in vivo* at discrete time points following laser irradiation which initiated BPD- and Photofrin-mediated PDT. Use of ODT provided quantitative structural features with high resolution, which has the potential for elucidating the mechanism(s) relevant to PDT.

Several authors have shown that vascular damage associated with PDT is a prerequisite for tumor regression. Our observations are consistent with studies describing PDT effects on vasculature, based on different techniques [13]–[20]. Using intravital microscopy on rats treated 24 h after Photofrin injection, Fingar *et al.* [15] observed transient constriction of 20–30-μm diameter arterioles during PDT, though at a higher light dose than used in the present study. They hypothesized that effects on microvasculature such as thrombus formation and vasoconstriction leading to blood flow stasis are induced by prostaglandins and also by thromboxane A_2 which is secreted from platelets through the action of ROS on the membranes of leukocytes, platelets and endothelial cells. The significance of the thromboxane mechanism was illustrated by the diminished vasoconstriction observed in thrombocytopenic rats [16].

Another mechanism, however, must be invoked to explain the rapid and complete recovery, accompanied by overshoot, of arterial diameter and blood flow velocity shortly after PDT. The measurements in the present study are in agreement with observations by Fingar *et al.* [15] on vessel diameter. Gilissen *et al.* [25] studied isolated rat aortas *ex vivo* and found that the endothelium derived relaxing factor (EDRF) was impaired by PDT. The endothelium is sensitive to ROS and, therefore, plays a key role in primary events of PDT. Recently, Furchgott [34] identified nitric oxide (NO) as EDRF. NO is a potent vasodilator and inhibitor of platelet aggregation, which is continuously released by the vascular endothelium and diffuses into the plasma and the subendothelium. In vascular smooth muscle, NO locally stimulates the production of cyclic guanine monophosphate (cGMP), which induces smooth muscle cell relaxation. The NO-cGMP-dependent mechanism makes NO a potent physiological vasodilator and important in the maintenance of vascular perfusion [28], [29], [35]. Seccombe and Schaff [36] demonstrated that after cardiac ischemia and reperfusion, ischemia-induced ROS impaired the receptor-dependent complex specific to the NO synthase in endothelium. PDT also involves generation of ROS causing endothelial cell injury, which may exert similar local effects on the deactivation of the NO signal transduction pathway. Alternative mechanisms depending on impairment of systemic vasostimulators, such as norepinephrine and acetylcholine, in the splanchnic vasculature may be excluded because vessel

diameter and blood flow at locations adjacent to the irradiated region, both proximal and distal, were not affected. It may be concluded that diminished NO release results in unopposed thromboxane-induced local vasoconstriction and thrombus formation.

This in turn may explain our observations: at the lower light dose ($D = 12$ J/cm^2) there was, presumably, no loss of endothelial cells. When PDT irradiation was discontinued, the local impairment of NO production ceased and regenerated NO was again able to act as a potent vasodilator. Vasodilation induced reperfusion, which supplied the thrombosed region of the vessel with coagulation inhibitors and, through increased blood flow, diluted the activated clotting factors. In future studies, vessel harvesting and assaying for NO in the arteries and thrombus in veins will provide valuable experimental data to evaluate the NO hypothesis.

Analysis of post-irradiation effects with BPD (Fig. 4) shows a dramatic influence of Δt. For $\Delta t = 20$ min, $d_a(t)$ decreased by 80% followed by rebound with vasodilative overshoot for $t > 40$ min. This seems to suggest a biochemically triggered response rather than damage to endothelial cells of the vessel wall. According to our hypothesis, BPD adhered to the surface of the vascular wall where ROS interacted with the endothelium and impaired NO release, which caused vascular smooth muscle cell contraction. It should be noted that thromboxane A_2 formation [16], mediated by ROS, also contributed to vasoconstriction. The basically intact endothelium continued to generate NO and eventually abolished the vasoconstrictive spasm. Overshoot was probably a result of regenerated NO together with compensation of PDT-induced oxygen depletion in tissue [21]. Diminished effects at $\Delta t = 4$ and 7 h were due to progressive metabolism of BPD.

In interpreting Figs. 4 and 5 we identify "fast" and "slow" acting photosensitizers, respectively: the BPD half-life in plasma is $t_{1/2} =$ 10–20 min [3], [4] and for Photofrin $t_{1/2} =$ 5–8 h [37], [38]. Moreover, we distinguish between PDT protocols involving "short" ($\Delta t = 20$ min) and "long" ($\Delta t =$ 7–8 h) drug-light time intervals. In Fig. 4, the fast-acting BPD, at $\Delta t = 20$ min, was still confined to the vascular compartment and adherent to the endothelium. ROS generated by photoexcitation of the sensitizer inhibited NO synthase thus causing vasoconstriction in the artery. In contrast to the transient arterial effects, mediated by the NO-cGMP mechanism, the veins displayed permanent and complete occlusion. Veins possess a thin vessel wall with little smooth muscle, which is not able to contract/dilate as dynamically as in arteries. The diminished venous lumen diameter and blood flow observed is due to thrombus formation at the vessel wall [Fig. 2(c)]. Moreover, since venous blood pressure is low the thrombus is not as likely to be dislodged as compared to the arteries.

As a possible explanation for vasodilation we suggest that at $\Delta t = 7$ h, BPD had predominantly accumulated in fatty tissues such as the mesentery, which act as a reservoir for BPD that is being slowly depleted by the venous system. Seven hours after BPD administration, photoexcitation generated ROS mainly outside the vascular compartment, particularly around the vein. The ensuing injury, most likely stimulated an acute inflammatory response which was accompanied by a local engorgement of blood. The more rigid artery was less affected [Fig. 4(a)] than the distensible vein [Fig. 4(b)], which exhibited venodilation during the 60-min post-PDT observation time.

In contrast, the slow-acting Photofrin at $\Delta t = 20$ min, had not yet accumulated in the endothelium to a sufficient extent and inhibition of NO synthase was only partial. Photoexcitation at $\Delta t = 8$ h caused more pronounced vasoconstriction [Fig. 5(a)], whereas venodilation after long drug-light interval [Fig. 5(b)] occurred in a similar fashion as discussed above in connection with BPD [Fig. 4(b)].

With Photofrin at the higher light dose ($D = 48$ J/cm^2), the artery-vein pair displayed complete stasis (Fig. 6). In this case, the endothelial lining and its surrounding tissue were not only altered biochemically but also damaged which caused thrombosis and irreversible shut down. Because low ROS levels affect endothelium only transiently, low irradiation doses are inappropriate for clinical applications of PDT.

The data acquisition time of approximately five minutes (needed for scanning a vessel pair) in the present ODT instrumentation, precluded measurement of short-time ($\sim$s) transients in arterial diameter and flow. However, when elucidating PDT effects, vessel changes take place on the order of minutes [15], so that faster data acquisition is of secondary importance.

Recent advances by other investigators [39] allow for simultaneous structural and velocity image formation in approximately 20 s; in the near future, we anticipate Doppler images will be recorded at a 1-Hz frame rate or higher, enabling on-line monitoring. Technical improvements in future ODT instrumentation will allow real-time monitoring of pulsative events during PDT in vessels at 1–2 mm tissue depths. We expect that blood flow reductions from pre-irradiation levels, as measured by ODT, can be related to the total levels of ROS which depend on the light and drug doses delivered to the vasculature. At low ROS levels, effects on the tumor vasculature are relatively minor and reversible; after laser irradiation is discontinued, reperfusion leads to a return of blood flow to pre-irradiation levels. High levels of ROS effectively destroy not only veins but also arteries leading to permanent ischemia; regional blood flow approaches zero and, after irradiation is discontinued, no recovery of pre-irradiation flow velocities is observed. A correlation of tissue necrosis due to vascular shut-down, as a function of drug and light doses, can then be carried out. The present study was limited to normal vasculature, but we expect similar PDT effects also to occur in tumor vasculature.

V. Conclusion

Noncontact tomographic imaging at discrete locations was performed with off-line analysis. The present study represents the first comprehensive use of ODT for measuring simultaneously microvascular changes and blood flow during PDT. We have measured PDT-induced changes in vessel diameter and mean flow velocity. ODT is thus an ideal technique for elucidating the mechanism(s) of clinical PDT for combating cancer and vascular disease.

REFERENCES

[1] T. J. Dougherty, "Photodynamic therapy," *Photochem. Photobiol.*, vol. 58, pp. 895–900, 1993.

[2] J. Moan and K. Berg, "Photochemotherapy of cancer: Experimental research," *Photochem. Photobiol.*, vol. 55, pp. 931–948, 1992.

[3] B. A. Allison, M. T. Crespo, A. K. Jain, A. M. Richter, Y. N. Hsiang, and J. G. Levy, "Delivery of benzoporphyrin derivative, a photosensitizer, into atherosclerotic plaque of Watanabe heritable hyperlipidemic rabbits and balloon-injured New Zealand rabbits," *Photochem. Photobiol.*, vol. 65, pp. 877–883, 1997.

[4] K. B. Trauner, R. Gandour-Edwards, M. Bamberg, S. Shortkroff, C. Sledge, and T. Hasan, "Photodynamic synovectomy using benzoporphyrin derivative in an antigen-induced model for rheumatoid arthritis," *Photochem. Photobiol.*, vol. 67, pp. 133–139, 1998.

[5] P. Ortu, G. M. LaMuraglia, W. G. Roberts, T. J. Flotte, and T. Hasan, "Photodynamic therapy of arteries: A novel approach for treatment of experimental intimal hyperplasia," *Circulation*, vol. 85, pp. 1189–1196, 1992.

[6] H. Kostron, A. Obwegeser, and R. Jakober, "Photodynamic therapy in neurosurgery: A review," *J. Photochem Photobiol Biol.*, vol. 36, pp. 157–168, 1996.

[7] B. W. Henderson. L. Vaughan, D. A. Bellnier, H. van Leengoed, P. G. Johnson, and A. R. Oseroff, "Photosensitization of murine tumor, vasculature and skin by 5-aminolevulinic acid-induced porphyrin," *Photochem Photobiol*, vol. 62, pp. 780–789, 1995.

[8] J. Leveckis, N. J. Brown, and M. W. Reed, "The effect of aminolaevulinic acid-induced, protoporphyrin IX-mediated photodynamic therapy on the cremaster muscle microcirculation *in vivo*," *British Journal of Cancer*, vol. 72, pp. 1113–1119, 1995.

[9] M. J. Hammer-Wilson, C. H. Sun, M. Ghahramanlou, and M. W. Berns, "*In vitro* and *in vivo* comparison of argon-pumped and diode lasers for photodynamic therapy using second-generation photosensitizers," *Lasers Surg. & Med.*, vol. 23, pp. 274–80, 1998.

[10] K. W. Woodburn. Q. Fan, D. Kessel, Y. Luo, and S. W. Young, "Photodynamic therapy of B16F10 murine melanoma with lutetium texaphyrin," *J. Investigative Dermatol.*, vol. 110, pp. 746–751, 1998.

[11] R. Hilf, "Cellular targets of photodynamic therapy," *Photodynamic Therapy. Basic Principles and Clinical Applications*, B. W. Henderson and T. J. Dougherty, Eds. New York: Marcel Dekker, 1992, pp. 47–54.

[12] I. Wang, S. Andersson-Engels, G. E. Nilsson, K. Wardell, and K. Svanberg, "Superficial blood flow following photodynamic therapy of malignant nonmelanoma skin tumours measured by laser Doppler perfusion imaging," *Br. J. Dermatol.*, vol. 136, pp. 184–189, 1997.

[13] W. M. Star, P. A. Marijnissen, A. E. van den Berg-Blok, J. A. C. Versteeg, and K. A. P. Franken, and H. S. Reinhold, "Destruction of rat mammary tumor and normal tissue microcirculation by hematoporphyrin derivative photoradiation observed *in vivo* in sandwich observation chambers," *Cancer Res.*, vol. 46, pp. 2532–2540, 1986.

[14] J. S. Nelson, L. H. Liaw, A. Orenstein, W. G. Roberts, and M. W. Berns, "Mechanism of tumor destruction following photodynamic therapy with hematoporphyrin derivative, chlorin, and phthalocyanine," *J. Nat. Cancer Inst.*, vol. 80, pp. 1599–1605, 1988.

[15] V. H. Fingar, T. J. Wieman, S. A. Wiehle, and P. B. Cerrito, "The role of microvascular damage in photodynamic therapy: the effect of treatment on vessel constriction, permeability, and leukocyte adhesion," *Cancer Res.*, vol. 52, pp. 4914–4921, 1992.

[16] V. H. Fingar, T. J. Wieman, and P. S. Haydon, "The effects of thrombocytopenia on vessel stasis and macromolecular leakage after photodynamic therapy using Photofrin," *Photochem. Photobiol.*, vol. 66, pp. 513–517, 1997.

[17] K. S. McMahon, T. J. Wieman, P. H. Moore, and V. H. Fingar, "Effects of photodynamic therapy using mono-L-aspartyl chlorin e6 on vessel constriction, vessel leakage, and tumor response," *Cancer Res.*, vol. 54, pp. 5374–5379, 1994.

[18] M. W. Reed, T. J. Wieman, D. A. Schuschke, and F. N. Miller, "A comparison of the effects of photodynamic therapy on normal and tumor blood vessels in the rat microcirculation," *Radiat. Res.*, vol. 119, pp. 542–552, 1989.

[19] V. Gottfried, R. Davidi, C. Averbuj, and S. Kimel, "*In vivo* damage to chorioallantoic membrane blood vessels by porphycene-induced photodynamic therapy," *J. Photochem. Photobiol. B: Biol*, vol. 30, pp. 115–121, 1995.

[20] C. Abels, R. M. Szeimies, P. Steinbach, C. Richert, and A. E. Goetz, "Targeting of the tumor microcirculation by photodynamic therapy with a synthetic porphycene," *J. Photochem. Photobiol. B: Biol*, vol. 40, pp. 305–312, 1997.

[21] B. J. Tromberg, A. Orenstein, S. Kimel, S. J. Barker, J. Hyatt, J. S. Nelson, and M. W. Berns, "*In vivo* tumor oxygen tension measurements for the evaluation of the efficiency of photodynamic therapy," *Photochem. Photobiol.*, vol. 52, pp. 375–385, 1990.

[22] V. H. Fingar and B. W. Henderson, "Drug and light dose dependence of photodynamic therapy: A study of tumor and normal tissue response," *Photochem. Photobiol.*, vol. 46, pp. 837–841, 1988.

[23] S. H. Selman and M. Kreimer-Birnbaum, P. J. Goldblayy, T. S. Anderson, R. W. Keck, and S. L. Britton, "Jejunal blood flow after exposure to light in rats injected with hematoporphyrin derivative," *Cancer Res.*, vol. 45, pp. 6425–6427, 1985.

[24] M. Kreimer-Birnbaum, G. M. Garbo, R. W. Keck, S. H. Selman, C. M. Foss, and B. M. Shiff, "Photodynamic therapy of tumors: Effects of hematoporphyrin derivative on normal rat intestine," *Cell Mol. Biol.*, vol. 40, pp. 915–923, 1994.

[25] M. J. Gilissen, L. E. A. van de Merbel-de Wit, W. M. Star, J. F. Koster, and W. Sluiter, "Effect of photodynamic therapy on the endothelium-dependent relaxation of isolated rat aortas," *Cancer Res.*, vol. 53, pp. 2548–2552, 1993.

[26] B. W. Henderson and T. J. Dougherty, "How does photodynamic therapy work?," *Photochem. Photobiol.*, vol. 55, pp. 145–157, 1992.

[27] X. J. Wang, T. E. Milner, and J. S. Nelson, "Characterization of fluid flow velocity by optical Doppler tomography," *Opt. Lett.*, vol. 20, pp. 1337–1339, 1995.

[28] Z. Chen, T. E. Milner, D. Dave, and J. S. Nelson, "Optical Doppler tomographic imaging of fluid flow velocity in highly scattering media," *Opt. Lett.*, vol. 22, pp. 64–66, 1997.

[29] Z. Chen, T. E. Milner, S. Srinivas, X. J. Wang, A. Malekafzali, M. J. C. van Gemert, and J. S. Nelson, "Noninvasive imaging of *in vivo* blood flow velocity using optical Doppler tomography," *Opt. Lett.*, vol. 22, pp. 1119–1121, 1997.

[30] Z. Chen, T. E. Milner, S. Srinivas, and J. S. Nelson, "Optical Doppler tomography: Imaging *in vivo* blood flow dynamics following pharmacological intervention and photodynamic therapy," *Photochem. Photobiol.*, vol. 67, pp. 56–60, 1998.

[31] B. A. J. Angelsen, *Waves, Signals and Signal Processing in Medical Ultrasonics*, vol. 1 and 2. Dept Physiol and Biomed Engineering. Trondheim: Norwegian Institute Science Technol, 1996.

[32] T. Lindmo, D. J. Smithies, Z. Chen, J. Stuart Nelson, and T. E. Milner, "Accuracy and noise in Optical Doppler tomography studied by Monte Carlo simulation," *Phys. Med. Bio.*, vol. 43, pp. 3045–3064.

[33] C. Upson, T. Faulhaber, D. Kamins, D. Schlegel, J. Vroom, R. Gurwitz, and A. van Dam, "The application visualization system: A computational environment for scientific visualization," *IEEE Comput. Graph. Applicat.*, vol. 9, pp. 30–42, 1989.

[34] R. F. Furchgott, The 1996 "Albert Lasker Medical Research Awards. The discovery of endothelium-derived relaxing factor and its importance in the identification of nitric oxide," *JAMA*, vol. 276, pp. 1186–1188, 1996.

[35] S. Moncada, "Nitric oxide in the vasculature: Physiology and pathophysiology," *Ann. NY Acad. Sci.*, vol. 811, pp. 60–67, 1997.

[36] J. F. Seccombe and H. V. Schaff, "Coronary artery endothelial function after myocardial ischemia and reperfusion," *Ann. Thorac. Surg.*, vol. 60, pp. 778–788, 1995.

[37] Q. Peng, J. Moan, M. Kongshaug, J. F. Evensen, H. Anholt, and C. Rimington, "Sensitizer for photodynamic therapy of cancer: A comparison of the tissue distribution of Photofrin I and aluminum phthalocyanine tetrasulfonate in nude mice bearing a human malignant tumor," *Int. J. Cancer*, vol. 48, pp. 258–264, 1991.

[38] F. A. Menezes da Silva and E. L. Newman, "Time-dependent photodynamic damage to blood vessels: Correlation with serum photosensitizer levels," *Photochem. Photobiol.*, vol. 61, pp. 414–416, 1995.

[39] J. A. Izatt, M. D. Kulkarni, S. Yazdanfar, J. K. Barton, and A. J. Welch, "*In vivo* bidirectional color Doppler flow imaging at picoliter blood volumes using optical coherence tomography," *Opt. Lett.*, vol. 22, pp. 1439–1441, 1997.

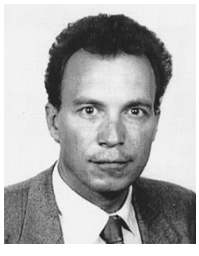

Attila Major was born in 1958 in Villach, Austria, and received the medical degree in 1984 at the University of Bern, Switzerland.

He has worked in primary hospitals and Universities since 1985 in Switzerland and Irvine, CA. His primary interests are in gynecologic oncology. At present, he is Associate Professor at the Department of Obstetrics and Gynecology, University Hospital of Geneva, Switzerland. He has published groundbreaking studies in the fields of hematology and photodynamic diagnosis and therapy.

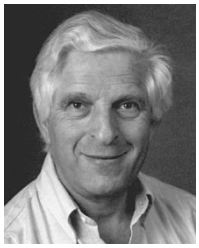

S. Kimel received the M.Sc. and Ph.D. degrees in chemistry from the University of Amsterdam, The Netherlands in 1955 and 1960, respectively.

He held a research associate position at the Weizmann Institute of Science, Rohovot, Israel, from 1955 to 1966. Currently, he is a Professor of Chemistry at the Technion—Israel Institute of Technology, Haifa 1966. He has held visiting academic appointments at numerous institutions: these include, Princeton University, Max-Planck Institute for Quantum Optics, Universite Paris-Nord, and the University of California at Irvine. His research interests span molecular spectroscopy; lasers and their applications in spectroscopy; photochemistry; photobiology; photomedicine; photodynamic therapy of cancer; and laser-tissue interactions.

Dr. Kimel is a corresponding member of the Royal Netherlands Academy of Arts and Sciences and in 1997 received Henry Taub Prize for Excellence in Research.

Steven Mee was born in 1972 in Long Beach, CA. He received the B.S. degree at the University of California, Irvine, in 1995 and the M.D. degree in 1999.

He has completed research in the oncological applications of lasers since 1996 and is currently completing a residency appointment at the Neuropsychiatric Institute, University of California at Irvine.

Thomas E. Milner, for photograph and biography, see this issue, p. 1066.

Derek J. Smithies received the B.Sc. degree with honors in theoretical physics in 1989, and the Ph.D. degree in medical physics in 1995. The objective of his Ph.D. work was to develop an automated system to scan copper vapor laser light over a port-wine stain to achieve the desired therapeutic effect.

Post-Doctoral work was carried out at the Beckman Laser Institute and Medical Clinic, Irvine, CA, to develop computer models to simulate the noninvasive measurement of blood vessel position and size in port-wine stains. He is currently at Indranet-Technologies Ltd., New Zealand, developing a wireless communication system for significantly higher bandwidth than the existing telephone network.

Shyam M. Srinivas, for photograph and biography, see this issue, p. 1141.

Zhongping Chen, for photograph and biography, see this issue, p. 1141.

J. Stuart Nelson, for photograph and biography, see this issue, p. 1066.